International Journal of Control
Publication details, including instructions for authors and subscription information:
http://www.tandfonline.com/loi/tcon20

Sliding mode scheme for adaptive specific growth rate control in biotechnological fed-batch processes

E. Picó-Marco [a] , J. Picó [b] & H. De Battista [c]

[a] Deptartment of Systems Engineering and Control , Technical University of Valencia , Spain

[b] Institute of Automation and Industrial Informatics , Technical University of Valencia , Spain

[c] Faculty of Engineering , National University of La Plata , Argentina

[d] Institute of Automation and Industrial Informatics , Technical University of Valencia , Spain E-mail:

Published online: 20 Feb 2007.

To cite this article: E. Picó-Marco , J. Picó & H. De Battista (2005) Sliding mode scheme for adaptive specific growth rate control in biotechnological fed-batch processes, International Journal of Control, 78:2, 128-141, DOI: 10.1080/00207170500073772

To link to this article: http://dx.doi.org/10.1080/00207170500073772

International Journal of Control
Vol. 78, No. 2, January 2005, 128–141

Sliding mode scheme for adaptive specific growth rate control in biotechnological fed-batch processes

E. PICÓ-MARCO†, J. PICÓ‡* and H. DE BATTISTA§

†Deptartment of Systems Engineering and Control, Technical University of Valencia, Spain
‡Institute of Automation and Industrial Informatics, Technical University of Valencia, Spain
§Faculty of Engineering, National University of La Plata, Argentina

(*Received 15 June 2004; revised 17 January 2005; accepted 19 January 2005*)

This paper addresses the control of biomass growth rate in fed-batch bioreactors. The main difficulty when designing controllers for these processes is the lack of accurate on-line knowledge of the controlled variable as well as the strong parameter and model uncertainties. A completely novel approach to the control design is introduced in this paper which allows us to overcome these problems. In fact, the proposed controller, which is applicable to a large class of fermentation processes, requires minimal knowledge of the process parameters and only uses on-line measurement of volume and biomass concentration. First, a reference model is proposed and a goal manifold in the state space is derived where the control objective is satisfied. A partial state feedback law is then proved to be an invariant control for the goal manifold. Then, the feedback gain is dynamically adjusted via a discontinuous action that enforces a sliding regime such that all state trajectories are steered towards the goal manifold. This sliding mode controller presents very attractive robustness properties. The performance of the controller is evaluated through numerical analysis and experimental results.

1. Introduction

Fed-batch processes are extensively used in the expanding biotechnological industry. The requirements to optimize the production and improve the product quality obtained from the bioreaction processes are encouraging the development of robust and reliable controllers. For this reason, fed-batch process control is receiving great attention by the research community. From the control viewpoint, fed-batch fermentation processes are a challenging problem. The control designer must deal with strong modeling approximations, parameter uncertainties, external disturbances, nonlinear and possibly non-minimum phase dynamics, lack of accurate on-line measurements of important variables involved in the process, etc.

A fed-batch bioreactor can be defined as a tank with no outgoing flow, where several microbial growth and enzyme-catalyzed reactions occur simultaneously in a liquid medium. The growth of biomass (bacteria, yeasts, etc.) proceeds by consumption of nutrients or substrates (carbon, nitrogen, oxygen, etc.) provided the environmental conditions (pH, temperature, illumination, etc.) are favorable. Simultaneously, some reactants are transformed into products or metabolites through the enzyme-catalyzed reactions mentioned above.

Most of the biotechnological processes treated here are pure cultures with one limiting substrate.[1] In many of these processes, the formation of the metabolite we are interested in is directly associated to microbial growth. These so-called growth-linked reactions are represented by Bastin and Dochain (1990) and Zlateva (2000).

$$S(\text{substrate}) \curvearrowright X(\text{biomass}) + P(\text{product}) \qquad (1)$$

The symbol $\curvearrowright$ indicates that the biomass is an autocatalyst. The more biomass there is, the more biomass (and product) can be produced. This growth may be inhibited by the presence of a certain product (an inhibitor) or an exceedingly high substrate concentration.

*Corresponding author. Email: jpico@ai2.upv.es

[1]Although the biomass needs several substrates to grow, only one is not in excess at a given production phase.

International Journal of Control
ISSN 0020–7179 print/ISSN 1366–5820 online © 2005 Taylor & Francis Group Ltd
http://www.tandf.co.uk/journals
DOI: 10.1080/10.1080/00207170500073772

Processes for the production of single-cell proteins, alcohol and gluconic acid all belong to this category (Zlateva 2000).

When developing models for control purposes, a set of standard simplifications are commonly performed (Dunn *et al*. 2003):

- The microorganisms are regarded as *black boxes*, without delving into the intracellular mechanisms (the model is said to be non-structured).
- The model is built supposing an average microorganism (it is said to be non-segregated).
- The conditions and concentrations in the tank are supposed to be homogeneous.
- Only the limiting substrate takes part in the model.
- Only one product is generally considered in the model: either the metabolite of interest or, if it exists, the inhibitor.

From a biological standpoint, an important goal is to force and keep microorganisms into a given physiological state in which production of a certain species is optimal (Jobé *et al*. 2003 and Henson and Seborg 1992). This specification usually translates into the following control objective: the regulation of the biomass growth rate.

The survey papers (Parulekar and Lim 1985, Johnson 1987, Lee *et al*. 1999, Rani and Rao, 1999), describe the history and state of the art in the field of fed-batch processes control. Due to the difficulties in measuring the controlled variable, many papers found in literature basically propose open-loop control with given feeding flow profiles. In many contributions proposing closed-loop control, the controlled variable is indirectly estimated by on-line measurements of some auxiliary variable such as dissolved oxygen and/or deal with very particular processes in which the substrate or a product is measurable. Two approaches are typical, either the substrate, the inhibitor product or the dissolved oxygen are regulated to a prefixed value, or a fixed feedforward exponential feeding is applied along with some error feedback term (Valentinotti *et al*. 2003, Oliviera *et al*. 2004, Arndt and Hitzmann 2004). Another research line is dedicated to develop more generic control strategies applying ideas of adaptive and optimal control (Smets *et al*. 2002, 2004). These control strategies employ an estimation of the controlled variable obtained from on-line measurement of biomass concentration (Claes and Van Impe 1999), a closed loop version of the exponential feeding law and some error feedback term. Although much progress has been made, this approach still presents some shortcomings to overcome. In fact, the sensitiveness to the high level of noise corrupting the estimation and the strong dependence on process parameters hamper the implementation of these controllers in real processes. Thus, for non-monotonous kinetic functions, the feedback gain switches according to the sign of the estimated growth rate derivative so as to globally stabilize the process. As a consequence of the high sensitivity to the noise corrupting the estimation, convergence to the desired set-point may be critically delayed in some circumstances. To cope with process uncertainties, some authors have suggested the use of neural network adaptive control and found it superior under some conditions to conventional adaptive control (Boscovic and Narendra 1995). In Moya *et al*. (2002), another approach to controller design with few measured variables is proposed which is based on the transformation of the process dynamics to the feed-forward form. Unfortunately, most of the published papers poorly evaluate the performance of the controllers under the realistic assumption of parameter uncertainty and corroborate their theoretical results by simulation analysis using simple mathematical models with known parameters.

In this paper, a novel controller for specific growth rate regulation is developed which is applicable to a large set of fermentation processes, in particular to those described by (1) with both monotonous and non-monotonous (with inhibition by substrate) growth kinetics. First, the control objective is stated in terms of a goal manifold (§ 2). An invariant control law is derived next (§ 3). Then, with the aim of having control of the reaching trajectory towards the goal manifold, and to robustify the controller against parameter uncertainties, a globally stabilizing adaptive algorithm is developed based on variable structure control theory and the associated sliding regimes (Sira-Ramirez 1988, Utkin 1992, Hung *et al*. 1993). The proposed sliding mode controller presents very interesting features. Most importantly, it assumes minimal knowledge of the process parameters and only requires on-line measurements of volume and biomass concentration.[2] Moreover, no estimator for the specific growth rate is used. Additionally, the controller completely rejects actuator (valves) errors and is robust to process parameter uncertainties and bounded disturbances in environmental variables. Particularly, zero steady state error is achieved despite all these types of perturbations as well as despite a biomass measurement offset. All these properties are corroborated by simulation (§ 5) and

[2]A biomass sensor (Navarro *et al*. 2001) that works accurately and reliably for a wide range of concentrations has been designed and patented by our research group. To obtain the experimental results presented in § 6, the proposed controller has used the data supplied by this sensor.

experimental results (§6). Finally, §7 outlines the conclusions of the paper and suggests future work.

2. Problem statement

Most of the fermentation processes represented by (1) have the following description in state-space (Bastin and Dochain 1990 and Dunn *et al*. 2003):

$$\Sigma_0 = \begin{cases} \dot{x} = \mu(s)x - Dx \\ \dot{s} = -y_s\mu(s)x - mx + D(s_i - s) \\ \dot{p} = y_p\mu(s)x - Dp \\ \dot{v} = F \end{cases} \tag{2}$$

where x, s and p are the biomass, substrate and product concentrations respectively; s_i is the influent substrate concentration; v is the volume; F is the feeding flow; $D = F/v$ is the dilution rate; y_s and y_p are yield coefficients; m is the maintenance constant. Finally, μ is the specific growth rate which is an either monotonous or non-monotonous function of substrate concentration. Typical examples are (figure 1):

- Monod:

$$\mu(s) = \frac{\mu_m s}{k_s + s} \tag{3}$$

- Haldane:

$$\mu(s) = \frac{\mu_o s}{k_s + s + (s^2/k_i)}. \tag{4}$$

The control objective is the regulation of this specific growth rate at a given value $\mu = \mu_r$.

Since p affects neither microbial growth nor substrate consumption, it has no influence on the controller design. Consequently the equation for product will be discarded. System Σ_0 with its third equation omitted will be hereinafter referred as Σ.

It should be noted the control specification implies that a given manifold must be tracked, i.e. it is not desired to stabilize around a point. Furthermore, the state trajectory on this manifold is unbounded. Volume goes to infinity, biomass concentration follows a bounded trajectory and only substrate concentration stabilizes around a value s_r satisfying $\mu(s_r) = \mu_r$.

The control design is subject to the following constraints:

- The only on-line measurable variables are volume and biomass concentration.
- The yield coefficient y_s, the maintenance constant m, and the influent substrate concentration s_i are uncertain parameters that, moreover, may vary during the process.
- The specific growth rate μ is an imprecisely known function of s.
- The control signal is the feeding flow F ($F \geq 0$).

Let us define a reference model for Σ:

$$\Sigma_r \triangleq \begin{cases} \dot{x} = \mu_r x - \lambda x^2, & x(t_0) = x_{r,0} \\ \dot{v} = \lambda x v, & v(t_0) = v_{r,0} \\ s = s_r. \end{cases} \tag{5}$$

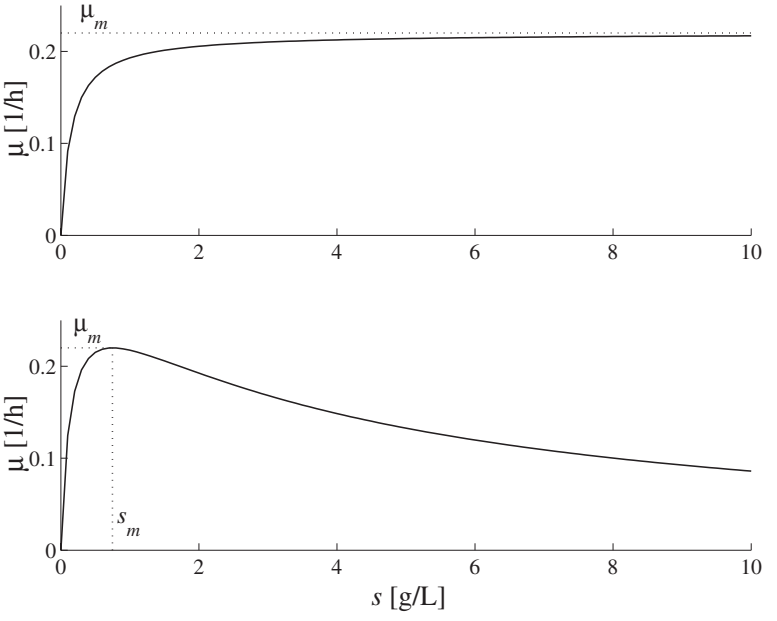

Figure 1. (a) Monod and (b) Haldane kinetic functions.

It can be shown (Picó-Marco and Picó 2003) that, no matter the form of μ, there exists an invariant control for Σ with respect to a reference manifold generated by Σ_r. In other words, once the state of Σ is on the reference manifold, it remains there.

This result is presented in the following section. Thereafter a sliding mode adaptive controller, which provides very interesting robustness properties, is developed using as basis the invariant control.

3. Invariant control

In order to get an explicit expression for the reference manifold, it must be noticed that the first equation in (5) is a logistic one, with solution:

$$x(t) = \frac{(\mu_r/\lambda)}{1 + ((\mu_r/\lambda x_{r,0}) - 1)e^{-\mu_r t}}. \tag{6}$$

The volume trajectory is easily obtained after realizing that the absolute biomass (xv) follows an exponential trajectory and $\dot{v} = \lambda(xv)$. Hence

$$v(t) = v_{r,0} + \frac{\lambda x_{r,0} v_{r,0}}{\mu_r}(e^{\mu_r t} - 1). \tag{7}$$

Solving (6) and (7) for t and equating, an integral for $\Sigma_{r\{x,v\}}$ is obtained:

$$x - \frac{\mu_r}{\lambda} - \left(x_{r,0} v_{r,0} - \frac{\mu_r}{\lambda} v_{r,0}\right)\frac{1}{v} = 0 \tag{8}$$

which, along with

$$s - s_r = 0 \tag{9}$$

defines the goal manifold, referred in the sequel as $Z_{r,0}$. Actually, there are different goal manifolds for different initial conditions $(x_{r,0}, v_{r,0})$. Figure 2 shows $Z_{r,0}$ for several initial conditions of the reference model. Note that the control objective of maintaining a constant growth rate μ_r is accomplished on any of these manifolds. In fact, what really matters is the slope of the manifolds. The difference among all these manifolds lies on the amount of biomass obtained at the end of the process.

A new coordinate system is obtained that has one coordinate z along $Z_{r,0}$ and two other coordinates φ_1, φ_2 transversal to it. The new coordinates can be defined as:

$$\left.\begin{aligned} \varphi_1 &\triangleq x - \frac{\mu_r}{\lambda} - (x_{r,0} v_{r,0} - \frac{\mu_r}{\lambda} v_{r,0})\frac{1}{v} \\ \varphi_2 &\triangleq s - s_r \\ z &\triangleq xv. \end{aligned}\right\} \tag{10}$$

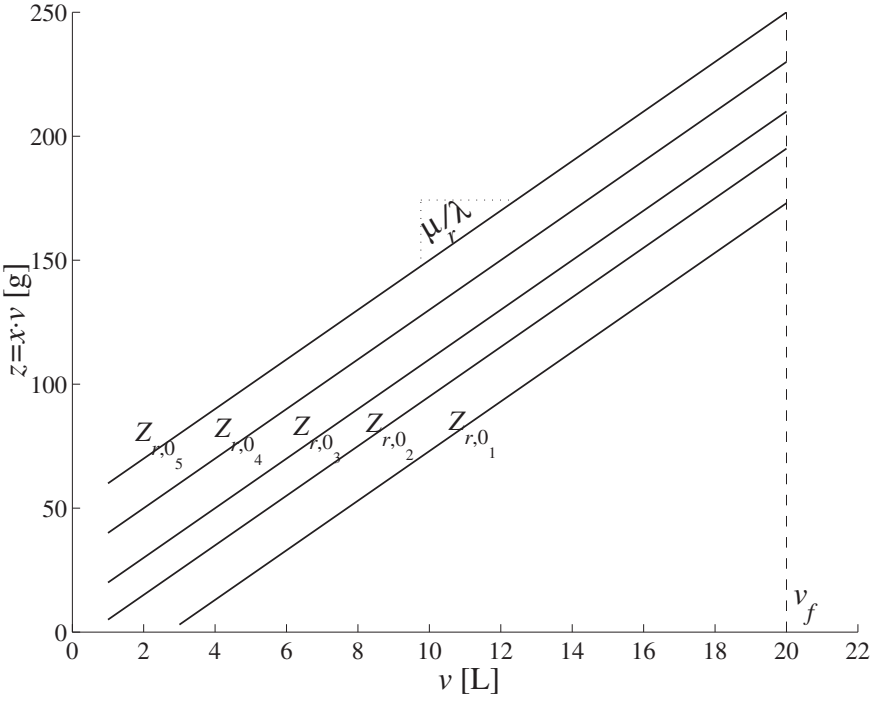

Figure 2. Goal manifolds on the $z - v$ plane.

Now, it must be confirmed that there exists an invariant control. That is, a control such that once the state of Σ reaches $Z_{r,0}$, it remains there, i.e. $\varphi = \mathrm{col}(\varphi_1, \varphi_2) \equiv 0$. The condition for (f, g)-invariance of a dynamic system $\dot{\boldsymbol{x}} = f(\boldsymbol{x}) + g(\boldsymbol{x})u$ with respect to the submanifold Z implies the existence of a solution $u = U(\boldsymbol{x})$ (the invariant control) of the algebraic equation

$$\frac{\partial \varphi}{\partial \boldsymbol{x}} f(\boldsymbol{x}) + \frac{\partial \varphi}{\partial \boldsymbol{x}} g(\boldsymbol{x}) u = 0 \quad \boldsymbol{x} \in Z. \tag{11}$$

In our case, two equations are obtained. The first one is fulfilled for the partial state feedback law:

$$F \triangleq U(x, v) = \lambda x v \tag{12}$$

for any constant λ. The second one gives an expression for λ:

$$\lambda = \lambda_r = \frac{y_s \mu_r + m}{s_i - s_r}. \tag{13}$$

Observation 1: Feedback laws similar to (12) can be found in the literature (see for instance Lee *et al.* (1999), Smets *et al.* (2004), Moya *et al.* (2002)). The expression (12) is derived here from a completely different approach. From equation (11), following Fradkov *et al.* (1999), it is easy to show that equations (12) and (13) constitute an invariant control for Σ on $Z_{r,0}$.

Observation 2: Given μ_r and hence λ, the biomass at the end of the process z_f (which is usually a variable of interest) is completely determined by the initial conditions of the reference model $(x_{r,0}, v_{r,0})$. From (8), it follows that $z_f = z_{r,0} + (\mu_r/\lambda)(v_f - v_{r,0})$ where $z_{r,0} = x_{r,0} v_{r,0}$ and v_f is the final volume of the reactor.

Observation 3: It is straightforward to demonstrate that (12)–(13) also provides local convergence towards a goal manifold $Z_{r,0}$ with unknown initial condition $(x_{r,0}, v_{r,0})$. Moreover, this convergence is global for monotonous kinetic functions, and also for Haldane-like functions provided s_i is properly bounded. For the sake of brevity, we omit this demonstration. Instead, we will demonstrate convergence of the robust sliding mode adaptive controller.

4. Sliding mode adaptive control

Let us consider process Σ with the partial feedback law (12):

$$\Sigma_f = \begin{cases} \dot{x} = \mu(s)x - \lambda x^2 \\ \dot{s} = -y_s \mu(s)x - mx + \lambda x(s_i - s) \\ \dot{v} = \lambda x v. \end{cases} \tag{14}$$

The problem to face now is the following. For any given initial conditions $(x_{r,0}, v_{r,0})$ defined for the reference model Σ_r, and any (not necessarily known) initial condition for the process Σ_f,[3] define an adaptive law for λ so that Σ_f is immersed into Σ_r with minimal knowledge of the kinetic function $\mu(s)$ and the process parameters.

Since only biomass and volume are assumed to be measured on-line, only the first off-the-manifold coordinate φ_1 will be used in the sequel as error signal. More specifically the normalized error signal:

$$\sigma(z, v, \lambda) \triangleq \frac{\varphi_1}{x} = 1 - \frac{z_{r,0}}{z} - \frac{\mu_r}{\lambda z}\left(v - v_{r,0}\right). \tag{15}$$

4.1. *Ideal sliding mode adaptation law*

The goal is to adapt λ so that $\sigma \to 0$ and thus system Σ_f approaches the zero level set of the integral of Σ_r defined by (8) despite process uncertainties. For this purpose, let us propose the following reaching dynamics for the nominal system (Hung *et al.* 1993, Sira-Ramirez 1993):

$$\dot{\sigma} = -N_1 \sigma - N_0 \,\mathrm{sign}\,(\sigma) \tag{16}$$

with $N_0 > 0$, $N_1 > 0$, so that the manifold $\sigma \equiv 0$ is reached in a finite time τ, ideally

$$\tau = \frac{1}{N_1} \ln\left(1 + \frac{N_1}{N_0} |\sigma(t_0)|\right).$$

Moreover, once the manifold defined by $\sigma \equiv 0$ is reached, the state trajectory will be ideally maintained on it by means of an infinite frequency switching action. This type of behaviour is called ideal sliding regime on the sliding manifold $\sigma \equiv 0$ (Sira-Ramirez 1988, Utkin 1992).

Differentiating (15):

$$\dot{\sigma} = \frac{\dot{\lambda}}{\lambda^2} \frac{v - v_{r,0}}{z} \mu_r + \mu(s)(1 - \sigma) - \mu_r \tag{17}$$

and equating to (16), the following discontinuous adaptation law for λ results:

$$\dot{\lambda} = \frac{-\lambda^2 z}{\mu_r \left(v - v_{r,0}\right)} [(N_1 - \hat{\mu})\sigma + N_0 \,\mathrm{sign}\,(\sigma) + \hat{\mu} - \mu_r]. \tag{18}$$

Actually, a precise estimation of μ ($\hat{\mu}$) is not necessary. This is one of the main advantages of the proposed control scheme. In fact, any bounded error in the

[3]For technical reasons, the initial volume of Σ_r must be chosen smaller than the one of Σ_f.

estimation of μ will be compensated by the linear and discontinuous feedback terms $N_1\sigma$ and $N_0\,\mathrm{sign}(\sigma)$ respectively. Furthermore, it is sufficient to choose $\hat{\mu} = \mu_r$. Conditions for N_0 and N_1 to impose an ideal sliding regime on $\sigma \equiv 0$ despite replacing $\hat{\mu}$ by μ_r can be easily derived (Sira-Ramirez 1988, Utkin 1992).

4.2. *Real sliding mode adaptation law*

We are interested in the implementation of the proposed control strategy. With this purpose, the infinite switching frequency that characterizes the ideal sliding mode should be limited. Actually, there are several approximations to the ideal sliding mode. For instance, the sign$(\cdot)$ function can be replaced by a pulse width modulator, a hysteresis comparator, a high-gain amplifier with saturation, etc. (Hung *et al.* 1993). In this paper, the latter approach has been taken which leads to a smooth control action (Slotine and Li 1991).

Let us redefine the adaptation law as:

$$\dot{\lambda} = \frac{-\lambda^2 z}{\mu_r(v - v_{r,0})}\, g(\lambda - \bar{\lambda},\, -\sigma)\left(\frac{1}{T_\sigma} - \mu_r\right)\sigma. \tag{19}$$

Assume for the moment that $g(\lambda - \bar{\lambda},\, -\sigma) \equiv 1$. Besides,

$$\frac{1}{T_\sigma} = \frac{N_0}{\max\{|\sigma|, \delta\}} + N_1 \tag{20}$$

$$N_0 = \nu(1 + n_0) \qquad n_0 > 0 \tag{21}$$

$$N_1 = \nu(1 + n_1) \qquad n_1 > 0 \tag{22}$$

$$\nu = \max\{\mu_r, \mu_m - \mu_r\} \tag{23}$$

with $0 < \delta < 1$.

Let us evaluate now the convergence of the real sliding mode control to the sliding manifold. From (17) and (19) the time evolution of the normalized error signal, i.e. the reaching dynamics is governed by:

$$\dot{\sigma} = -\left[\frac{1}{T_\sigma} + \mu(s) - \mu_r\right]\sigma + (\mu(s) - \mu_r). \tag{24}$$

Define now the Lyapunov-like function:

$$W = \frac{1}{2}\sigma^2. \tag{25}$$

Then:

$$\begin{aligned}\dot{W} &= -\frac{N_0}{\max\{|\sigma|, \delta\}}\sigma - N_1\sigma^2 + (\sigma - \sigma^2)(\mu - \hat{\mu}) \\ &= \begin{cases} (\mu - \mu_r)\sigma - N_0|\sigma| - (N_1 + \mu - \mu_r)\sigma^2 & |\sigma| \geq \delta \\ (\mu - \mu_r)\sigma - \left(\dfrac{N_0}{\delta} + N_1 + \mu - \mu_r\right)\sigma^2 & |\sigma| < \delta \end{cases} \\ &< 0 \quad \text{for } |\sigma| > \frac{\delta}{1 + n_0 + n_1\delta}. \end{aligned} \tag{26}$$

Notice that, although μ_r has been used instead of an estimation of μ, the off-the-manifold error can be done arbitrarily small by appropriately selecting the constant δ and the gains n_0 (N_0) and n_1 (N_1).

Observation 4: In the limit, choosing $\delta \to 0$, the real sliding mode adaptation law converges to the ideal sliding mode previously described.

4.3. *Stability analysis*

It has been already shown that state trajectories converge to (the close vicinity of) $\sigma \equiv 0$. This section is devoted to demonstrate that system trajectories on the sliding surface $\sigma \equiv 0$ asymptotically converge to the goal manifold $Z_{r,0}$. In other words, we will demonstrate that if the first off-the-manifold error (φ_1) is maintained at zero, the second off-the-manifold error (φ_2) also tends to zero (i.e. $s \to s_r$) and the feedback gain tends to its nominal value λ_r given by (13). Besides, the biomass concentration converges to a given trajectory whereas volume diverges (according to (6) and (7), respectively). In the case of non-monotonous kinetics some precautions must be taken.

4.3.1. Sliding dynamics. On the sliding manifold $\sigma \equiv 0$, the closed-loop system dynamics (14) can be rewritten as follows:

$$\Sigma_\sigma = \begin{cases} \dot{s} = [-y_s\mu(s) - m + \lambda(s_i - s)]x \\ \dot{\lambda} = \left[-\lambda^2\,\dfrac{\mu(s) - \mu_r}{\mu_r}\,\dfrac{v}{v - v_{r,0}}\right]x \\ \dot{v} = [\lambda v]x \end{cases} \tag{27}$$

where the equation for λ has been obtained from (17) and the sliding mode existence condition ($\sigma = 0$, $\dot{\sigma} = 0$). Besides, the equation for biomass concentration has been omitted to avoid redundancy. In fact, on the sliding manifold $\sigma \equiv 0$, x is algebraically dependent on the other state variables: $x = (z_{r,0}/v) + (\mu_r/\lambda v)(v - v_{r,0})$. See that replacing x in the last equation of (27) yields $\dot{v} = \mu_r(v - v_{r,0}) + \lambda z_{r,0}$, which

confirms that the volume diverges exponentially on $\sigma \equiv 0$ (recall that $v_0 > v_{r,0}$).

4.3.2. Partial stability

Definition: Let $\Psi : \mathcal{V} \triangleq [v_0, \infty[\mapsto]1, \psi_0]$ the function $\psi(v) = (v/v - v_{r,0})$. See that $v = \psi^{-1}(\psi) = v_{r,0}(\psi/\psi - 1)$ and that the Frechet derivative $\psi' = -(\psi - 1)^2/v_{r,0}$. Furthermore, x can be rewritten as $x = \left[x_{r,0}(\psi - 1) + \mu_r/\lambda\right](1/\psi)$.

Definition: Let ζ the partial state $\zeta = \mathrm{col}(s, \lambda)$ and $\zeta_r = \mathrm{col}(s_r, \lambda_r)$. Recall that $s \in \mathcal{S} =]0, s_i[$ and $\lambda \in \Re^+$. Let $\mathcal{M} = \mathcal{S} \times \Re^+$, and M_σ the region of $\sigma \equiv 0$ such that $\zeta \in \mathcal{M}$.

Let define the continuously differentiable function

$$V(\zeta, \psi) = \psi \int_{s_r}^{s} \frac{\mu(\varsigma) - \mu_r}{\mu_r} \mathrm{d}\varsigma + (s_i - s_r)\left[\ln \frac{\lambda}{\lambda_r} + \frac{(\lambda_r - \lambda)}{\lambda}\right]. \tag{28}$$

with time derivative

$$\dot{V}(\zeta, \psi) = -\psi x(\zeta, \psi)\left[(\psi - 1)\lambda \int_{s_r}^{s} \frac{\mu(\varsigma) - \mu_r}{\mu_r} \mathrm{d}\varsigma + \frac{y_s}{\mu_r}(\mu(s) - \mu_r)^2 + \frac{\lambda}{\mu_r}(\mu(s) - \mu_r)(s - s_r)\right]. \tag{29}$$

Locally around ζ_r, $V(\zeta, \psi)$ is upper and lower bounded by the positive definite functions $\overline{V}(\zeta) \triangleq V(\zeta, \psi_0)$ and $\underline{V}(\zeta) \triangleq V(\zeta, 1)$:

$$\underline{V}(\zeta) \leq V(\zeta, \psi) \leq \overline{V}(\zeta). \tag{30}$$

Additionally,

$$\dot{V}(\zeta, \psi) \leq -Q(\zeta) \tag{31}$$

where $Q(\zeta) \triangleq -\dot{V}(\zeta, 1)$ is nonnegative definite.

Then, Σ_σ is Lyapunov stable with respect to ζ uniformly in v, and there exists $\mathcal{D} \subseteq \mathcal{M}$ $(\mathcal{D} \ni \zeta_r)$ such that for all $(\zeta, v) \in \mathcal{D} \times \mathcal{V}$, $\zeta(t) \to \mathcal{E}(\mathcal{D}) \triangleq \{\zeta \in \mathcal{D} : Q(\zeta) = 0\}$ as $t \to \infty$ (Chellaboina and Haddad 2002). Although it is not generally true for partially stable systems, an invariance principle can be derived for asymptotically autonomous partial systems (Chellaboina and Haddad 2002, Rouche *et al.* 1977) (Ch. 8). Fortunately, this is our case. In fact, $\psi \to 1$ and $x \to \mu_r/\lambda$ as v diverges. So, the partial system $\Sigma_{\sigma,\zeta}$ defined by the first two equations of (27) asymptotically converges to the autonomous system

$$\Sigma^a_{\sigma,\zeta} = \begin{cases} \dot{s} = [-y_s\mu(s) - m + \lambda(s_i - s)]\dfrac{\mu_r}{\lambda} \\ \dot{\lambda} = -\lambda(\mu(s) - \mu_r) \end{cases} \tag{32}$$

It is easy to see that ζ_r is the largest invariant set for (32) in $\mathcal{E}(\mathcal{D})$. Consequently, Σ_σ is asymptotically stable with respect to ζ uniformly in v.

4.3.3. Global stability for monotonous kinetic functions.

For monotonous kinetic functions, e.g. Monod,

* $V(\zeta, \psi)$ verifies (30) for all $\zeta \in \mathcal{M}$ and $\underline{V}(\zeta)$ is radially unbounded.
* $\dot{V}(\zeta, \psi)$ verifies (31) for all $\zeta \in \mathcal{M}$ and ζ_r is the largest invariant set for (32) in $\mathcal{E}(\mathcal{M})$.

Consequently, Σ_σ is globally asymptotically stable with respect to ζ_r uniformly in v (Chellaboina and Haddad 2002). Then, the system Σ_f on $\sigma \equiv 0$ globally asymptotically converges to the goal manifold $Z_{r,0}$ defined by the reference model Σ_r.

4.3.4. Stability for non-monotonous kinetic functions.

For non-monotonous kinetic functions, e.g. Haldane, the previous results about stability, and hence about convergence towards $Z_{r,0}$ are only local. Actually, the partial system may present two equilibrium points. Let us denote s_m the substrate concentration at which the growth rate is maximum, $s_r < s_m$ and $s^r > s_m$ the substrate concentrations satisfying $\mu(s_r) = \mu(s^r) = \mu_r$. Locally around s_r, the kinetic function behaves as a monotonous function. Then, Σ_σ locally asymptotically stabilizes around ζ_r uniformly in v, and the system Σ_f on $\sigma \equiv 0$ locally asymptotically converges to the goal manifold $Z_{r,0}$.

In the sequel, the adaptation law is modified in order to achieve global convergence towards $Z_{r,0}$.

Definition: Let $\mathcal{S}^r = \{s \in \mathcal{S} : s < s^r\}$, $\mathcal{L}^r = \{\lambda \in \Re^+ : \lambda < \lambda^r = (y_s\mu_r + m)/(s_i - s^r)\}$, $\mathcal{M}^r = \mathcal{S}^r \times \mathcal{L}^r$ and M^r_σ the region of $\sigma \equiv 0$ where $\zeta \in \mathcal{M}^r$.

It is clear from (29) and (27) that M^r_σ is a domain of attraction of ζ_r on the sliding manifold $\sigma \equiv 0$, that is a region of convergence towards $Z_{r,0}$ on $\sigma \equiv 0$. Nevertheless, if the adjustable feedback gain λ or the substrate concentration take large values, the system state might reach (the close vicinity of) the sliding manifold outside the domain of attraction, leading to undesired unstable dynamics.

A possible solution suggested here is to modify the adaptation law so that the trajectories are steered to reach the attractive region M^r_σ of the sliding manifold $\sigma \equiv 0$. A natural way of avoiding the aforementioned

undesired dynamics is limiting the feeding governed by λ and s_i.

Let rewrite the second equation of Σ_f, where, to simplify the analysis, the stabilising term $-mx$ is disregarded:

$$\dot{s} = [-y_s\mu(s) + \lambda(s_i - s)]x. \tag{33}$$

Figure 3(a) displays a Haldane kinetic function μ(s) and the reference growth rate. Let assume we fix $\lambda = \bar{\lambda}$ with $\lambda_r < \bar{\lambda} < \lambda^r$. The solid straight line represents the equation $y = \bar{\lambda}(s_i - s)/y_s$. Note that for all values of s such that the curve μ(s) is over the solid line, the right hand side of (33) is negative, that is s decreases. As a consequence, the partial state ζ will reach $\mathcal{M}^r$ and will remain there until $\sigma \equiv 0$ (specifically, M_σ^r) is eventually reached. According to this, the adaptation law is modified by incorporating the saturation function

$$g(w_1, w_2) = \begin{cases} 0 & \text{if } w_1 \geq 0 \wedge w_2 \geq 0 \\ 1 & \text{otherwise.} \end{cases} \tag{34}$$

To complete the analysis, we need to show that despite saturation, all state trajectories finally reach the vicinity of $\sigma \equiv 0$. In fact, during λ saturation ($\dot{\lambda} = 0$), the first term of (17) is cancelled. Then, the derivative of the Lyapunov-like function (25) becomes

$$\dot{W} = -\mu\sigma^2 + (\mu - \mu_r)\sigma. \tag{35}$$

On one hand, if $\sigma > 0$, saturation becomes inactive ($g(\cdot,\cdot) = 1$) and the right-hand side of (18) is negative (i.e. λ leaves saturation). Thus, inequality (26) holds, i.e. the trajectory points towards $\sigma \equiv 0$. On the other hand, if $\sigma < 0$, λ remains at its limit value. Therefore, to approach $\sigma \equiv 0$, (35) should be negative whenever $\sigma < 0$. It can be shown that this is true, possibly except for an initial period of time. In fact, as λ is maintained fixed at $\bar{\lambda}$, the partial state ζ will finally reach $\mathcal{M}^r$, and moreover, will converge to $\bar{\zeta} = (\bar{s}, \bar{\lambda}) \in \mathcal{M}^r$, where $\bar{s}$ is the substrate concentration at which the solid line crosses the kinetic function in figure 3(a). Since $\mu(\bar{s}) > \mu_r$, $\dot{W}$ will, sooner or later, become negative. Consequently, trajectories will finally point towards $\sigma \equiv 0$ from both sides as desired.

Observation 5: Note, however, that limiting λ is not sufficient to guarantee global attraction towards $\mathcal{M}^r$. In fact, consider figure 3(b) that corresponds to a larger value of s_i. In this case, although $\lambda_r < \bar{\lambda} < \lambda^r$, $\mathcal{S}^r$, and hence $\mathcal{M}^r$, is not reached from all initial conditions. In particular, it is not so from large initial substrate concentrations. This means that s_i should also be limited. In fact, the line must be below the μ(s)

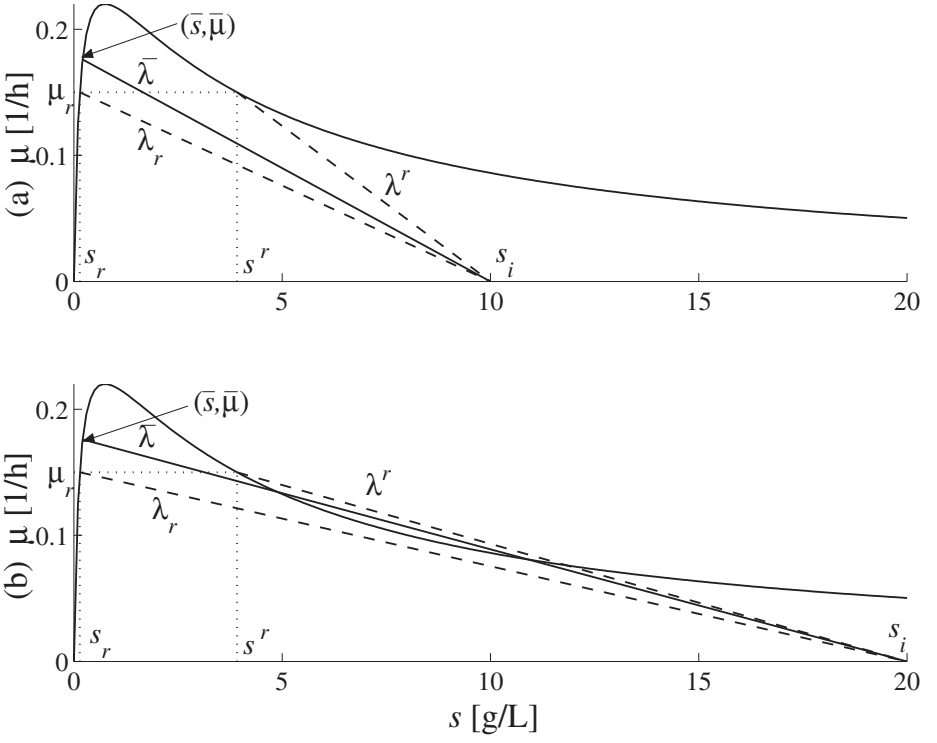

Figure 3. Limit value of gain λ for Haldane-like kinetics.

curve for $s \in \mathcal{S} - \mathcal{S}^r$. Unfortunately, the more uncertain the kinetic function is, the more conservative the design should be.

Observation 6: Note that for Monod-like kinetic functions, although it is not necessary to assure convergence toward $Z_{r,0}$, limiting λ may also be used to improve the transient from certain initial conditions. Certainly, a kind of windup effect may appear due to the saturation of Monod functions and the integrator implicit in (18). Then, in order to reach and maintain the process state on the sliding manifold $\sigma \equiv 0$, a large overshoot in λ may appear, leading to an excess of feeding and a large settling time. Limiting appropriately the value of λ, the substrate concentration is bounded hence avoiding strong saturation of the growth rate and the associated windup effect. Based on the previous analysis, global convergence towards $Z_{r,0}$ on the sliding manifold $\sigma \equiv 0$ is still guaranteed despite λ limitation provided $\bar{\lambda} > \lambda_r$.

4.4. *Robustness properties*

The proposed control strategy presents very attractive robustness features. Note that the control signal $F = \lambda x v$ and the adaptation law (19) are completely insensitive to the system parameter uncertainties. In fact, neither y_s, nor m, nor the equilibrium substrate concentration s_r are used to compute the control signal. For the same reason, the control strategy is not affected by perturbations in the influent substrate concentration s_i. Furthermore, no on-line estimation of the substrate concentration or the specific growth rate is used by the control algorithm. In the case of non-monotonous kinetics, only some bounds for the process parameters are needed to design the limit value of λ (along with an adequate value for s_i), thus guaranteing global stability. In order to have a criteria to design the sliding mode gains N_0 and N_1, just an upper bound for the maximum achievable value of μ is necessary. When properly designed, these gains N_0 and N_1 enforce the state towards the vicinity of the sliding manifold $\sigma \equiv 0$ despite the lack of knowledge of μ and the process parameters, and despite uncertainties in the actuators (valves) response (the valves can be seen as within a high gain loop, so that any error in F leads to a negligible error in σ).

On the other hand, to compute the off-the-manifold error signal σ which governs the gain adaptation law, as well as the control signal F, both biomass concentration and volume must be measured. Nevertheless, it is easy to see that a biomass concentration measurement offset does not affect the steady state growth rate. In fact, replacing λ by F/z in (15), where F is the real control action, it follows that the off-the-manifold error σ becomes independent of z (and also of x) as biomass increases ($z \gg z_{r,0}$). Moreover, a steady state growth rate offset (i.e. an off-the-manifold error) can only be caused by errors in volume measurement.

5. Simulation results

Simulation results for fed-batch processes with both Monod and Haldane kinetics are presented to corroborate the attractive features of the proposed control strategy.

The process and controller parameters used in simulations are listed in table 1. The Monod and Haldane kinetic functions are depicted in figure 1.

5.1. *Monod kinetics*

Here, the ability to regulate the growth rate μ at its desired value μ_r despite noisy (with zero mean) measures of x and v, and despite uncertainties in the process parameters k_s, y_s and m is evaluated. These uncertainties cause an error in the nominal initial condition $\lambda_0 = \lambda_r$. The simulation results for initial conditions $(x_0, s_0, v_0) = (x_{r,0}, 0.1, v_{r,0}{}^+)$ are presented in figure 4. The nominal response of the system, i.e. when the parameters are assumed to be perfectly known, is drawn in solid line. It is observed that the growth rate μ and the adaptable gain λ rapidly converge towards their desired values μ_r and λ_r, respectively. Simulation results have been also obtained when a +100% error in the estimation of k_s is considered in the controller design. The time response under this test condition is overlapped by the nominal response. Additionally, the dashed line depicts the performance with a +20% error in the estimation of y_s. Finally, with dot-dashed line, the response neglecting the maintenance constant m in the determination of λ_0 is shown. In all cases, the closed-loop responses rapidly converge towards the nominal response, corroborating

Table 1. Parameters and test conditions.

Parameter	Value	Parameter	Value
μ_m [1/h]	0.22	v_f [L]	30
k_s [g/L]	0.14	μ_r [1/h]	0.1
y_s	1.43	s_i [g/L]	20
m [1/h]	0.05	δ	0.05
k_i [g/L]	4	ν_0	0.5
$x_{r,0}$ [g/L]	5	ν_1	0.5
$v_{r,0}$ [L]	$\lesssim 1$		
Meas. noise x	$+\{-0.1, 0, 0.1\}x$		
Meas. noise V	$+\mathcal{N}(0.5, 0.01)$ $+\mathcal{N}(0, 0.001)$		

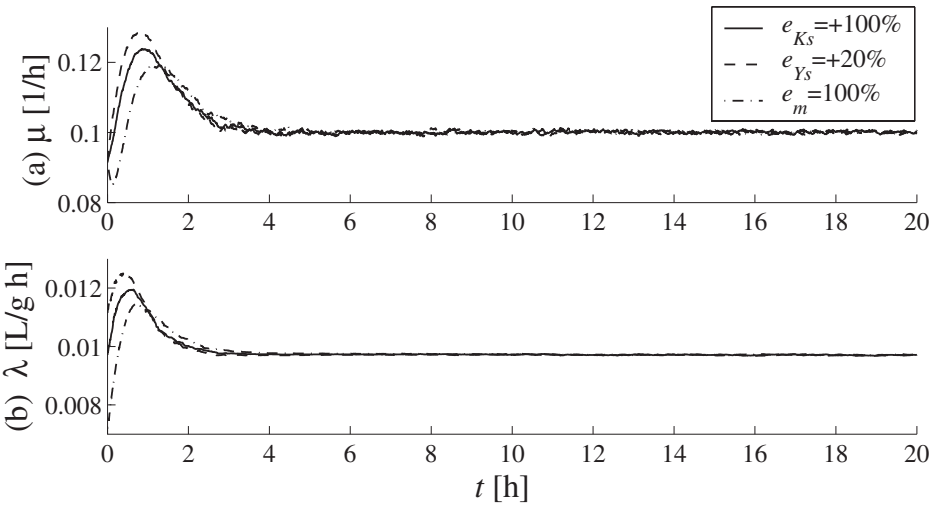

Figure 4. Simulation results (first 20 hours) for Monod kinetics with parameter uncertainties.

the excellent regulation properties despite parameter uncertainties and measurement noise.

5.2. *Haldane kinetics*

In this subsection different simulation results are presented for a fed-batch process with Haldane kinetics.

Figure 5 shows in solid line the response of the closed-loop system for initial conditions beyond its peak value ($s > s_m$): $(x_0, s_0, v_0) = (x_{r,0}, 2.5, {v_{r,0}}^+)$. It is seen that the substrate concentration is rapidly reduced and, consequently, the growth rate converges to its desired value μ_r. Simulation results are also presented when a $\pm 10\%$ error in the biomass measurement is considered (dashed and dot-dashed lines). Note that the adjustable gain λ tends to different steady state values (figure 5(b)) to compensate for these large errors in the measured biomass (figure 5(c)). As a consequence, the growth rate is stabilized at μ_r, corroborating the robustness property to biomass measurement errors.

Finally, simulation analysis were conducted to validate the ability of the controller to reach the prescribed manifold from different initial conditions (figure 6). The response from $(x_0, s_0, v_0) = (x_{r,0}, 0.1, {v_{r,0}}^+)$ is drawn in solid line. The prescribed surface is immediately reached and the growth rate rapidly converges to μ_r. The response from a larger initial biomass concentration ($x_0 = 1.4 \cdot x_{r,0} = 7\text{g/L}$) is shown in dashed line. The excess of biomass and the low incoming flow (low λ) necessary to reduce the normalized error σ lead to the undershoot in the growth rate observed in figure 6(a). After the prescribed surface is reached, the growth rate rapidly converges to its desired value. On the other hand, the response from an initial condition with negative error σ is depicted in dotted line. The system state converges towards the prescribed surface with a velocity governed by the controller parameters n_0 and n_1. The incoming flow (i.e. λ) is increased to reduce the magnitude of this error. Unfortunately, when the prescribed manifold is reached, $\lambda \gg \lambda^r$, and the state trajectory is oriented in opposite direction to the domain of attraction M_σ^r. Consequently, both the controller parameter λ and the substrate concentration s diverge. Conversely, the response of the system from the same initial condition but bounding the gain $\lambda \leq \bar{\lambda}$ is shown in dot-dashed line. At the cost of enlarging the reaching time, this limitation of the feedback gain guarantees that the prescribed manifold is reached inside the domain of attraction of the equilibrium point for the partial state $\zeta = \zeta_r$.

Observation 6: The simulation results using large initial errors σ shown in this last example are intended to put in evidence the reaching and stabilizing properties of the proposed controller. In practice, however, the initial conditions for x and v of process Σ and of reference system Σ_r can be adjusted to avoid large transient responses.

6. Experimental results

In this xsection some experimental results are presented. A fed-batch fermentation on glucose is included, carried out using the natural *Saccharomyces cerevisiae* strain $T_{73}wt$ and medium YPD. The goal was to keep a low specific growth rate $\mu_r = 0.11\text{h}^{-1}$ so as to avoid the formation and accumulation of ethanol. Environmental conditions where controlled to $T = 30°\text{C}$ and $pH = 4.5$ on a Biostat B5L reactor.

The experimental results are shown in figure 7. After an initial batch with a glucose concentration of 5g/L, the controlled fed-batch was switched on at $t_0 = 7.65\text{h}$,

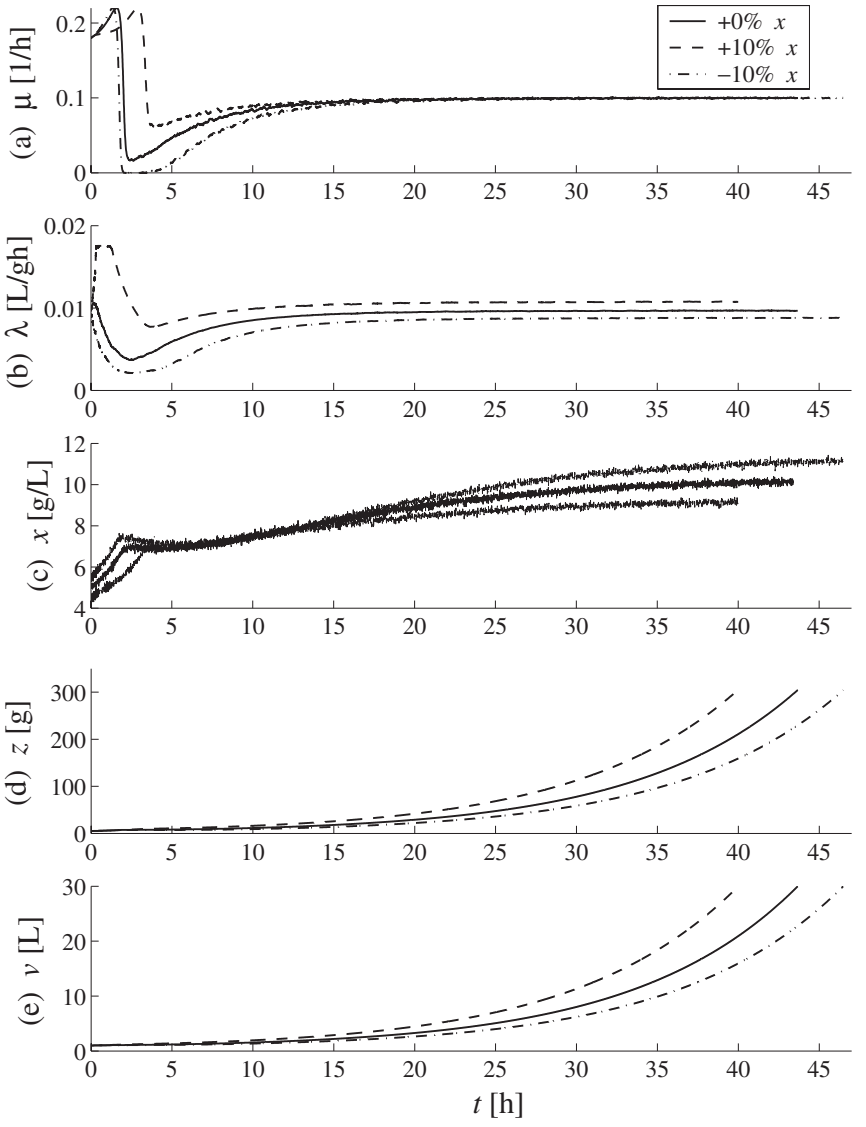

Figure 5. Simulation results for Haldane kinetics with biomass error measurement.

when the glucose in the medium was almost depleted. The concentration of glucose in the feeding flow was set to 20g/L. The constants of the goal manifold were set to $z_{r,0} = z(t_0)$ and $v_{r,0} = 0.9v(t_0)$, whereas the initial value of the feeding gain λ was set to $\lambda(t_0) = 1.3 \cdot 10^{-3}\mathrm{L(gh)}^{-1}$. Under these conditions, the initial value of the normalized off-the-manifold error results $\sigma(t_0) = -2.3$.

The control algorithm increases λ (figure 7(c)) in order to approach the sliding surface $\sigma \equiv 0$ (figure 7(b)). The integral action inherent to the controller causes an initial overshoot in the specific growth rate for some 4 hours (figure 7(a)). This transient overshoot could have been reduced by choosing $z_{r,0}$, $v_{r,0}$ and $\lambda(t_0)$ so that $\sigma(t_0) \cong 0$. Anyway, the large initial value of $\sigma(t_0)$ allows us to corroborate the reaching properties towards $\sigma \equiv 0$ of the algorithm. During the rest of the experiment, the specific growth rate μ keeps around the desired value but for some periods of time (around $t = 20\,\mathrm{h}$ and $t = 25\,\mathrm{h}$). At these, μ drops due to limitation in the oxygen supply, as seen in figures 7(d) and 7(e) looking at the decrease of pO_2 at $t = 20\,\mathrm{h}$ and the increase of the stirrer speed at $t = 25\,\mathrm{h}$. This behaviour occurs because there was deficient control loop for pO_2 in the experiment, and O_2 was not considered as a limiting substrate in the model. Actually, whenever this limitation appears, one should improve the oxygen transfer rate by means of the air supply and stirrer speed and/or demand for a lower specific growth rate. The long term variation in λ (figure 7(c)), which is commonly observed in all long experiments, can be explained as an adaptation to the varying yield

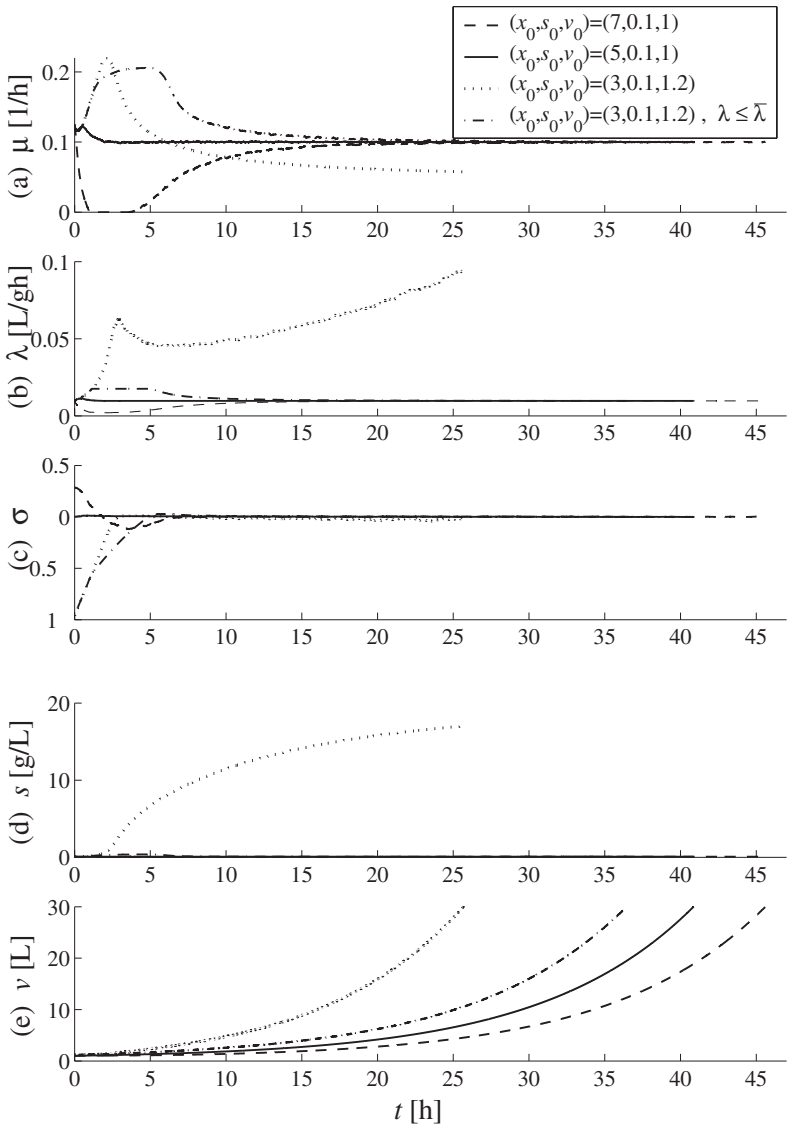

Figure 6. Simulation results for Haldane kinetics from different initial conditions.

coefficient y_s. For this reason, control strategies using a-priori estimation of y_s usually fail to regulate the specific growth rate during the whole experiment.

Figure 7(f) shows the evolution of the absolute biomass w.r.t. volume. Also, goal manifolds for different representative values of λ are depicted. These values of λ were obtained at the beginning ($t = 8$h), the middle ($t = 20$ h) and the end ($t = 35$ h) of the fed-batch process. Recall that the appropriate value of the feeding gain λ is not known and even varies with time. Therefore, the goal manifold must also be searched for, as it depends on λ. Notice how, after the transient phase, the absolute biomass z follows a trajectory parallel to the goal manifold $Z_{r,0,\lambda(35\text{h})}$. The reason why the trajectory tracks a parallel to $Z_{r,0,\lambda(35\text{h})}$ instead of $Z_{r,0,\lambda(35\text{h})}$ itself is due to an offset in the measurement of the off-the-manifold error. Yet, the controller is robust against this kind of offsets. Thus, the specific growth rate is correctly driven to the reference.

Finally, it is important to stress the low values of glucose in the medium after the initial batch. They kept at values around 0.023g/L throughout the experiment. Their order of magnitude is close to that of measurement noise. Therefore, a control strategy based somehow on measurements or estimation of the substrate is not feasible in practice. As for the ethanol concerns, the low specific growth rate avoided its formation.

7. Conclusions and further research

In this paper, an SM-based adaptive controller was developed for specific growth rate regulation of a large class of fermentation processes. The main advantage

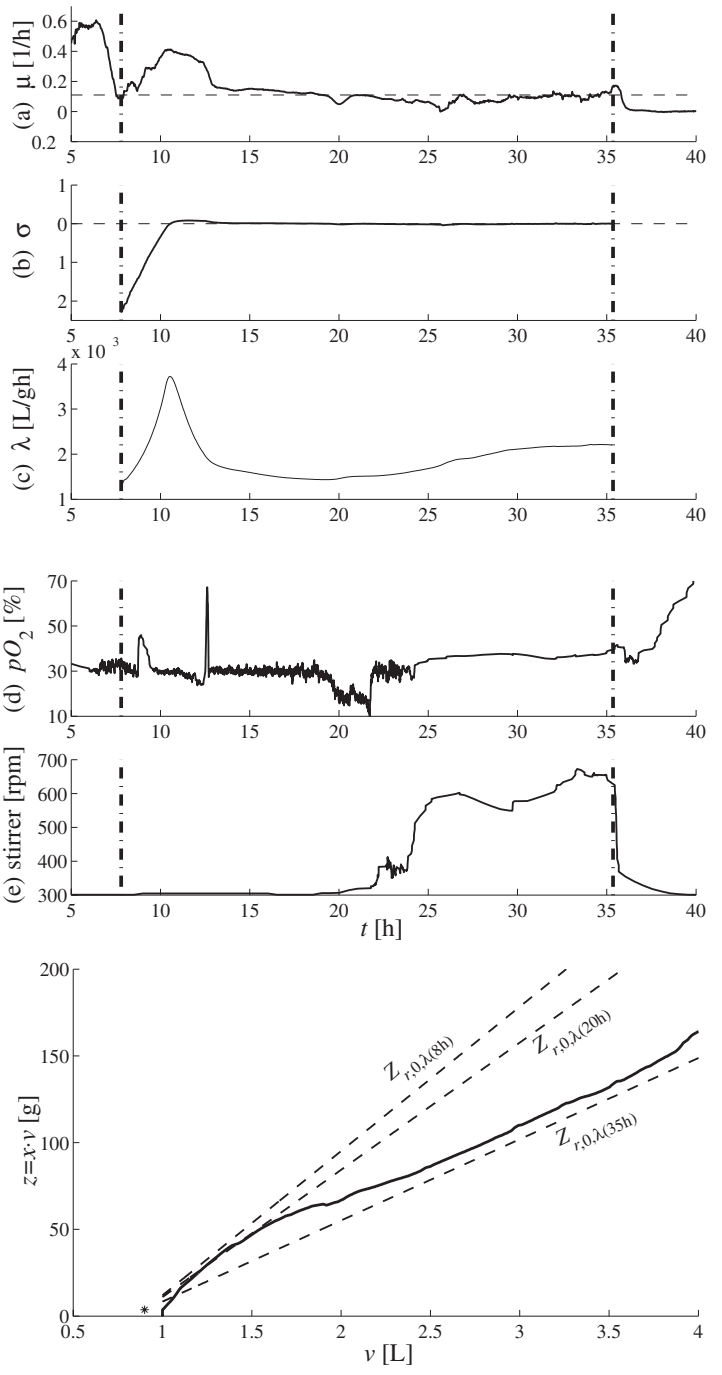

Figure 7. Experimental results for the fed-batch fermentation on *S. cerevisiae* T_{73}.

of this controller is that requires minimal knowledge of the process under control, thus presenting strong robustness properties to parameter uncertainties. Moreover, zero steady state error is achieved despite these uncertainties as well as despite biomass measurement errors. These attractive features are corroborated by simulation and experimental results. The control law is applicable to fed-batch processes with monotonous kinetics as well as non-monotonous ones with substrate inhibition. Further research should be oriented to extend these results to other types of fermentation processes, for instance those with product inhibition. In this case a new actuator could be introduced which separates a fraction of the inhibitory product from the broth Gonzalez-Vara *et al.* 2000). This would account for introducing a new term of the form $-(\alpha/v)p$ in product equation of Σ_0. It can be shown that this new control action, along with the existing one, form again an

invariant control. Measuring the product an analogous adaptive scheme should be analized, as an alternative to schemes trying to regulate the inhibitory product to a residual value (Valentionotti *et al*. 2003).

Acknowledgment

This research has been partially supported by the European Union through the network NACO2 (HPRN CT 1999 00046) and the Spanish Government (CICYT DPI2002-00525). The first two authors work with an Associated Unit to the Department of Biotechnology at the Institute of Agrochemistry and Food Technology (IATA) of the National Research Council (CSIC). The third author is member of CONICET. The experiments were carried out at the facilities of Biopolis S.L.

References

M. Arndt and B. Hitzmann, ''Kalman Filter Based Glucose Control at Small Set Points during Fed-batch Cultivation of *Sacccharomyces cerevisiae*'', *Biotechnology Progress*, 20, pp. 377–383, 2004.

G. Bastin and D. Dochain, *On-line Estimation and Adaptive Control of Bioreactors*, Amsterdam, Netherlands: Elsevier, 1990.

J. Boscovic and K. Narendra, ''Comparison of linear, nonlinear and neural-network-based adaptive controllers for a class of fed-batch fermentation processes'' *Automatica*, 31, pp. 817–840, 1995.

V. Chellaboina and W. Haddad, ''A unification between partial stability and stability theory for time-varying systems'', *IEEE Control Systems Magazine*, 6, pp. 66–75, 2002.

J. Claes and J. van Impe, ''On-line estimation of the specific growth rate based on viable biomass measurements: experimental validation'' *Bioprocess Engineering*, 21, pp. 389–395, 1999.

I. Dunn, E. Heinzle, J. Ingham and J. Přenosil, *Biological Reaction Engineering. Dynamic Modelling Fundamentals with Simulation Examples*, Germany: Wiley-VCH Verlag, 2003.

A.L. Fradkov, I.V. Miroshnik and V.O. Nikiforov, *Nonlinear and Adaptive Control of Complex Systems*, Dordrecht, Netherlands: Kluwer, 1999.

A. Gonzalez-Vara, G. Vaccari, E. Dosi, A. Trilli, M. Rossi and D. Matteuzzi, ''Enhanced production of $1-(+)-$lactic acid in chemostat by *Lactobacillus casei* DSM 20011 using ion-exchange resins and cross flow filtration in a fully automated plant controlled via nir'' *Biotechnology and bioengineering*, 67(2), pp. 147–156, 2000.

M. Henson and D. Seborg, ''Nonlinear control strategies for continuous fermenters'', *Chemical Engineering Science*, 47, pp. 821–835, 1992.

J. Hung, W. Gao and J. Hung, ''Variable structure control: a survey'', *IEEE Trans. Industrial Electronics*, 40, pp. 2–22, 1993.

A. Jobé, C. Herwig, M. Surzyn, B. Walker, I. Marison and U. von Stockar, ''Generally applicable fed-batch culture concept based on the detection of metabolic state by on-line balancing'', *Biotechnology and Bioengineering*, 82, pp. 627–639, 2003.

A. Johnson, ''The control of fed-batch fermentation processes – A survey'', *Automatica*, 23, pp. 691–705, 1987.

J. Lee, S. Lee, S. Park and A. Middelberg, ''Control of fed-batch fermentations'', *Biotechnology Advances*, 17, pp. 29–48, 1999.

P. Moya, R. Ortega, M. Netto, L. Praly and J. Picó, ''Application of nonlinear time-scaling for robust controller design of reaction systems'', *International Journal of Robust and Nonlinear Control*, 12, pp. 57–69, 2002.

J. Navarro, J. Picó, J. Bruno, E. Picó-Marco and S. Vallés, ''On-line method and equipment for detecting, determining the evolution and quantifying a microbial biomass and other substances that absorb light along the spectrum during the development of biotechnological processes'', Patent ES20010001757, EP20020751179, 2001.

R. Oliviera, R. Simutis and S. Feyo de Azevedo, ''Design of a stable adaptive controller for driving aerobic fermentation processes near maximum oxygen transfer capacity'', *Journal of Process Control*, 14, pp. 617–626, 2004.

S. Parulekar and H. Lim, ''Modeling, optimization and control of semi-batch bioreactors'', *Advances in Biochemical Engineering/Biotechnology*, 32, pp. 207–258, 1985.

E. Picó-Marco and J. Picó, ''Partial stability for specific growth rate control in biotechnological fed-batch processes'', *Proc. IEEE Conference on Control Applications* (CCA03), 2003.

K. Rani and V. Rao, ''Control of fermenters – A review'' *Bioprocess Engineering*, 21, pp. 77–88, 1999.

N. Rouche, P. Habets and M. Laloy, *Stability Theory by Lyapunov's Direct Method*, New York: Springer-Verlag, 1977.

H. Sira-Ramírez, ''Differential geometric methods in variable structure control'' *International Journal of Control*, 48, pp. 1359–1390, 1988.

H. Sira-Ramírez, ''On the dynamical sliding mode control of nonlinear systems'', *International Journal of Control*, 57, pp. 1039–1061, 1993.

J. Slotine and W. Li, *Applied Nonlinear Control*, Englewood Cliffs NJ: Prentice-Hall, 1991.

I. Smets, G. Bastin and J. van Impe, ''Feedback stabilization of fed-batch bioreactors: non-monotonic growth kinetics'', *Biotechnology Progress*, 18, pp. 1116–1125, 2002.

I. Smets, J. Claes, E. November, G. Bastin and J. van Impe, ''Optimal adaptive control of (bio)chemical reactors: past, present and future'' *Journal of Process Control*, 14, pp. 795–805, 2004.

V. Utkin, *Sliding Modes in Control and Optimization*, Berlin, Germany: Springer-Verlag, 1992.

S. Valentinotti, B. Srinivasan, U. Holmberg, D. Bonvin, C. Cannizzaro, M. Rhiel and U. von Stockar, ''Optimal operation of fed-batch fermentations via adaptive control of overflow metabolite'', *Control Engineering Practice*, 11, pp. 665–674, 2003.

P. Zlateva, ''Output stabilization of fermentation processes: a binary control system approach'', *Bioprocess and Biosystems Engineering*, 23, pp. 81–87, 2000.